Time-sequential Neuroinflammatory Response After Organophosphate-induced Status Epilepticus

Clémence Maupu
IRBA: Institut de recherche biomedicale des armees
Julie Enderlin
INSERM UMR1141: Neurodiderot
Alexandre Igert
IRBA: Institut de recherche biomedicale des armees
Stéphane Auvin
INSERM UMR1141: Neurodiderot
Rahma Hassan-Abdi
INSERM UMR1141: Neurodiderot
Nadia Soussi-Yanicostas
INSERM UMR1141: Neurodiderot
Xavier Brazzolotto
IRBA: Institut de recherche biomedicale des armees
Florian Nachon
IRBA: Institut de recherche biomedicale des armees
Grégory Dal Bo
IRBA: Institut de recherche biomedicale des armees
Nina Dupuis (ninadupuis@yahoo.fr)
Institut de recherche biomédicale des armées 1 Place Général Valérie André, BP 73 91223 Brétigny sur Orge cedex France https://orcid.org/0000-0003-3466-2152

Research

Keywords: Astrocyte, microglia, cytokines, seizure, diisopropylfluorophosphate, organophosphates, organophosphorus, SE

Posted Date: September 8th, 2020

DOI: https://doi.org/10.21203/rs.3.rs-72760/v1

Abstract

Background: Organophosphate compounds (OPs), either pesticides or chemical warfare agents are characterized by irreversible cholinesterase inhibition. In addition to severe peripheral symptoms, high doses of OPs can lead to seizures and status epilepticus (SE). Long lasting seizure activity and subsequent neurodegeneration promote neuroinflammation leading to profound pathological alterations of the brain. The aim of this study was to characterize neuroinflammatory responses at key time points after DFP-induced SE.

Methods: SE was induced by diisopropylfluorophosphate (DFP) injection in male Swiss mice. Immunohistochemistry (IHC) analyses of microglial (Iba1) and astrocytic (GFAP) cell markers were studied at 1, 4, 24 h and 3 days post-SE in the hippocampus. In parallel, using RT-qPCR, microglial and astrocytic phenotype markers were quantified on isolated CD11B (microglia) and GLAST (astrocytes)-positive cells after DFP-induced SE.

Results: At earlier stages (1-4 h) after SE, although IHC analysis presented no modification, an increase in pro-inflammatory (M1-like) markers and A2-specific markers was observed in CD11B and GLAST-positive isolated cells respectively. Microglial cells sequentially expressed immuno-regulatory (M2b-like) and anti-inflammatory (M2a-like) at 4 h and 24 h of SE induction. At later stages (24 h and 3 days), microglial and astrocytic activations were visible by IHC and Iba1-positive cells were increased in number in DFP animals compared to controls. Finally, at these later stages, A1-specific markers were increased in isolated astrocytes.

Conclusions: Our work identified sequential microglial and astrocytic phenotype activations. Although the role of each phenotype in SE cerebral consequences requires further study, targeting specific markers at specific time point could be a beneficial strategy for OP-induced SE treatment.

Background

Exposure to organophosphate compounds (OPs), widely used as chemical warfare agents and pesticides, represent a threat for both civilian and military communities. In addition to severe peripheral symptoms, high doses of OPs can elicit seizures that rapidly progress to status epilepticus (SE). SE is a life-threatening neurological emergency, characterized by continuous seizures without full recovery resulting in later neuronal damage, cognitive alterations and epileptogenesis [1]. OPs act as potent irreversible inhibitors of both central and peripheral cholinesterases (ChEs), resulting in acetylcholine accumulation and therefore uncontrolled activation of cholinergic receptors. Centrally, excessive activation at muscarinic receptors by acetylcholine can initiate extended seizures [2] evolving to self-sustained SE with the additional involvement of glutamatergic and GABAergic systems imbalance. The first-line treatment of OP poisoning consists of the injection of a muscarinic antagonist (e.g. atropine sulfate) combined with an oxime acting mainly as a peripheral ChE re-activator (e.g. pralidoxime or obidoxime). Additionally, the administration of an anticonvulsant (a benzodiazepine or a prodrug like avizafone) is currently

indicated in the early phase of OP poisoning in order to control seizures and SE. However, experimental data in line with clinical experience clearly show that approximately 30–40 min after the initial seizures, SE becomes refractory to benzodiazepines and classical anti-epileptic drugs [3]. In animal models, thirty minutes of unabated SE is also associated to severe seizure-related brain damage [4–7] and long-term consequences as epilepsy and cognitive decline [1].

Excitotoxic neuronal damage and seizure activity following SE development activate a neuroinflammatory response with marked microglia and astrocytes activations (7–10). Conversely, neuroinflammatory mechanisms have been implicated in SE-induced excitotoxic neuronal death, epileptogenesis and drug-resistance [8–11]. Reactive microglia and astrocytes can both have either protective or deleterious effects suggesting functional heterogeneity for both cell types. Based on *in vitro* experiments, microglia has been categorized into pro-inflammatory (M1-like), anti-inflammatory (M2a-like) and immuno-regulatory (M2b-like) subtypes [12–14]. Likewise, reactive astrocytes have also been recently differentiated in A1 and A2 phenotypes [15, 16]. Although the different subtypes are more likely a continuum with possibly numerous sub-classes, the different subtypes help our understanding of the complex neuroinflammatory mechanisms taking place after a neurological insult as SE.

We have recently developed and characterized a new convulsive mouse model of OP exposure using diisopropylfluorophosphate (DFP) [17]. In this model, DFP induces electrographic SE within 20 min and all seizing animals develop long-lasting SE. To study neuroinflammation in this model, we choose 4 key time points: 1 h after DFP injection corresponding to the onset of benzodiazepine resistance, 4 h corresponding to beginning of neuronal suffering observed by the marker FluoroJade C, 24 h corresponding to the peak of neurodegeneration and 3 days corresponding to early epileptogenesis.

Here, we show with histological techniques that DFP-induced SE is associated to microglia and astrocyte activations in the hippocampus. We choose to focus on the hippocampus given the crucial role of this structure in seizure development and epileptogenesis. We further characterize changes in microglial activation state with specific cell sorting followed by RT-qPCR, identifying sequential pro-inflammatory, immuno-modulatory and anti-inflammatory markers up-regulation beginning 1 hour after DFP exposure. Using the same technique, we observed that A2 astrocyte markers up-regulation precedes the A1 markers up-regulation. These data should help to understand microglial and astrocytic activations kinetics and adapt treatment paradigm in order to address the different phases of neuroinflammation and increase therapeutic impact.

Methods

Animals

Adult male Swiss mice (8 weeks, Janvier Labs, Le Genest-Saint-Isle, France) were housed four per cage with a 12 h/12 h light/dark cycle and food and water ad libitum. A period of 5–7 days of acclimation to housing conditions was observed. All animals were 9 weeks old when exposed to DFP. Animal

experiments were approved by the ethics committee according to applicable French legislations, in compliance with the “3Rs” policy of reduction, refinement and replacement of animal use for scientific procedures (Directive 2010/63/UE, décret 2013 – 118, approval number 9642-2017040316305252).

Drugs

DFP (Sigma Aldrich, L'Isle d'Abeau Chesnes, France) was freshly prepared by diluting the initial concentrated solution (0,1 g/ml in isopropanol) in ice-cold 0.9% (w/v) saline. The oxime HI-6 (1-2-hydroxy-iminomethyl-1-pyridino-2-oxanopropane) dichloride was a generous gift of DRDC Suffield (Canada). Atropine sulfate (AS, Sigma Aldrich, L'Isle d'Abeau Chesnes, France) and HI-6 were diluted in 0.9% (w/v) saline. Veterinary Diazepam (TVM, Lempdes, France) was used undiluted.

DFP exposure

The day of the experiment, mice received an injection of DFP (3 LD50 = 9.93 mg/kg, LD50 calculated without HI-6 and AS post-treatment, 10 ml/kg, s.c.) followed by combined i.p. injection of HI-6 (50 mg/kg) and AS (3 mg/kg) at + 1 min of DFP injection. HI-6 and AS post-treatment is used to reduce respiratory distress and mortality. As previously shown [17], the OP exposure protocol used in this project caused reduced mortality. In this project, the mortality rate in the DFP treated animals was < 10%, death occurring in the first 30 minutes after DFP injection. Protocol used for drugs administration is depicted in Fig. 1.

Except for the 1 h experimental group, all animals received Diazepam (10 mg/kg, i.p.), eighty minutes after DFP injection, corresponding to 1 h long SE. Diazepam was used to minimize the impact of SE on animal welfare and to homogenize SE duration between animals. Control animals received all treatments after vehicle injection without DFP.

Based on our previous work using electrocorticography in parallel of behavioral signs evaluation of seizing *vs* nonseizing animals [17], in this work observation of intoxication signs after DFP exposure allow to identify SE animals.

Immunofluorescence

After deep anesthesia, animals were transcardially perfused with 10 ml of 0.9% NaCl/5 UI/ml heparin, followed by 50 ml of 4% paraformaldehyde (PFA) in phosphate buffer. After overnight post-fixation in 4% PFA, brains were cryoprotected 24 h in 30% sucrose and then frozen 1 min in -40 °C isopentane. Thirty µm coronal sections were immunolabeled with anti-Iba1 (1:1000, Wako) and anti-GFAP (1:1000, Millipore) antibodies overnight at room temperature. Brain sections were then washed in PBS and subsequently incubated for 1 h at room temperature in 1:500 TRITC anti-rabbit IgG and 1:500 Alexa Fluor 488 anti-mouse IgG (Invitrogen). For each animal, analyses were conducted on images acquired at 3 rostrocaudal levels separated by 180 µm centered on Fig. 48 of Franklin and Paxinos mouse brain atlas (3rd edition). For each image, using Fiji software, regions of interest were delimited in the CA1, CA3 and dentate gyrus hippocampal regions. The same regions of interest were used for Iba1 cells counting and Iba1 and GFAP immunodensity evaluations. The final results were expressed as % of positive area and % of mean control values for Iba1 and GFAP immunodensities and in cells number/mm² for Iba1 cells counts.

Neural tissue dissociation and magnetic activated cell sorting

Brains were collected (1 animal per sorting) for cell dissociation and microglial cells and astrocytes were enriched using a magnetic-bead-coupled antibody (anti-CD11B and anti-GLAST respectively) extraction technique (MACS), as previously described and according to the manufacturer's protocol ([18]; Miltenyi Biotec, Bergisch Gladbach, Germany). In brief, after removing the cerebellum and olfactory bulbs, each brain was dissociated using the neural tissue dissociation kit. From the resulting brain homogenates, microglial cells were enriched by MACS using anti-CD11B microbeads, and after elution, isolated cells were centrifuged for 10 min at 300 g and conserved at -80 °C. Astrocytes were enriched by MACS using anti-GLAST microbeads on the remaining unretained cells and collected similarly to microglial cells. Microglial cells and astrocytes were sorted 1 h, 4 h, 24 h and 3 d after vehicle/DFP injection in control (n = 7–8 /time point) and DFP (n = 12–16/time point) mice.

RNA Extraction and RT-qPCR

Total RNA from isolated microglial cells and astrocytes were extracted with NucleoSpin ® RNA Plus XS kit according to the manufacturer's instructions (Macherey-Nagel, Hoerdt, France). Purified RNA quality and concentration were assessed by spectrophotometry using a NanoDropTM apparatus (Thermoscientific, Wilmington, DE). 200–400 ng of total RNA was subjected to reverse transcription using the IscriptTM cDNA synthesis kit (Bio-Rad, Marnes-la-Coquette, France). RT-qPCR was performed in triplicate for each sample on a CFX384 Real Time System (Bio-Rad), using SYBR Green Supermix (Bio-Rad) for 40 cycles. Amplification specificity was assessed by melting curve analysis. Primers were designed using Primer3 software and manufactured by Eurofins Genomics (Ebersberg, Germany). Primer sequences are summarized in Table S1. For expression analyses of CD11B-positive cells, for each sample, the expression of genes of interest was calculated relative to the expression of the reference gene TATA-box binding protein (*Tbp*). For expression analyses of GLAST-positive cells, for each sample, the expression of genes of interest was calculated relative to the expression of the reference gene ribosomal protein L13a (*Rpl13a*). The final results are presented as fold change over control mean values. Analyses were performed using Bio-Rad CFX Manager 3.0.

Statistical analysis

Data were analyzed using PRISM 7 software (GraphPad, San Diego, CA, U.S.A.). Data were expressed as means ± standard errors of the mean (SEM). Statistical comparison to control group was performed using the Mann-Whitney test. Sample sizes are indicated in figures.

Results

Microglial and astrocytic activations 1 hour after DFP exposure

To determine glial activation state at the time of SE drug refractoriness, we quantified microglial and astrocytic activations 1 h after DFP exposure, corresponding to 40 min of SE according to our previous report [17]. We first undertook an immunohistochemical (IHC) analysis of Iba1-positive microglia and GFAP-positive astrocytes. One hour after DFP injection, Iba1-positive cells number and Iba1 immunodensity were not statistically different in DFP SE animals and control animals in CA1, CA3 and DG (Fig. 2a-c). On the same animals, GFAP immunodensity was neither altered by SE (Fig. 2a and 2d). Given the intertwining of astrocyte processes, we were unable to quantified GFAP-positive cells number at any time point.

We further studied microglial and astrocytic activations using expression analysis of markers of polarized states. Gene expression analysis was performed after CD11B-positive (microglia/infiltrating macrophages) and GLAST-positive (astrocytes) cell sorting in DFP SE and control whole brains. In isolated CD11B-positive cells, quantitative RT-PCR experiments showed a differential increase of pro-inflammatory markers (*Il1b, Tnf*) but lack of immuno-regulatory (*Il1rn, Il4ra, Socs3*) and anti-inflammatory markers (*Lgals3, Mrc1, Igf1, Il10*) modulations (Fig. 2e). In GLAST-positive cells, quantitative RT-PCR experiments indicated an increase of A2-specific markers *Ptgs2* and *Ptx3*, as well as *Il6* cytokine mRNA but no A1-specific markers (*Serping1, Ggta1, Amigo2, H2-D1*) modifications (Fig. 2f).

Taken together, these findings indicate that 1 h after DFP injection, microglial cells very rapidly develop an activated state with a pro-inflammatory phenotype. Interestingly, in the same time, expression experiments on isolated astrocytes, allowed us to observe that astrocytes do not yet develop a neurotoxic A1-associated reactivity but an A2-associated reactivity associated to an *Il6* mRNA up-regulation. This is supported by the lack of pro-inflammatory cytokines *Ilb* and *Tnf* mRNA up-regulations in GLAST-positive cells.

Microglial and astrocytic activations 4 hours after DFP exposure

Going forward, we next studied microglial and astrocytic activations 4 h after DFP injection. The IHC analysis showed no modifications of Iba1-positive cells number and immunodensity (Fig. 3a-3c). Similarly, GFAP-positive astrocyte immunodensity was not different in DFP SE animals compared to control animals (Fig. 3a and 3d).

While no modifications were visible in histology, RNA expression analysis allowed us to identify a combined pro-inflammatory and immuno-regulatory markers up-regulations in CD11B-positive microglia/infiltrated macrophages, associated to an increase of the anti-inflammatory marker, *Lgals3* (Fig. 3e). In the same time, isolated GLAST-positive astrocytes developed a frank A2-associated phenotype with an up-regulation of *Emp1*, *S100a10* and *Cd109* A2-specific markers (Fig. 3f). As for the 1 h time point, this A2 activation state was associated to *Il6* mRNA increase. No A1-specific markers were modified as *Il1b* and *Tnf* mRNA (Fig. 3f).

These findings indicate that 4 h after DFP injection, in absence of clear morphological modifications that could be visualized by IHC immunodensity, microglia develop in parallel to a pro-inflammatory phenotype an immuno-regulatory phenotype. These experiments could not evaluate if these 2 activated states were present in the same microglial population or in 2 different cell populations. At the same time point, astrocytic activation state did not change from the 1 h time point, astrocytes strengthen their A2 phenotype associated with an *Il6* mRNA up-regulation. Interestingly, the A1 phenotype was also not observed at this time point.

Microglial and astrocytic activations 24 hours after DFP exposure

We have previously reported important neurodegeneration 24 h after DFP-induced SE [17]. At this time point, CA1, CA3 and DG hippocampal regions, as other brain regions, are affected by prominent neuronal damage. The IHC analysis uncovered an increase of Iba1 microglia/infiltrated macrophages cells number (Fig. 4a and 4b), as well as, an important increase of Iba1 immunodensity in CA1 and CA3 hippocampal regions (Fig. 4a and 4c). In these 2 regions, GFAP immunodensity was also increased (Fig. 4a and 4d). Conversely, also affected by brain damage at this time point [17], the DG region presented no elevation of Iba1, nor GFAP immunodensities.

These histologic modifications were associated for isolated CD11B-positive microglia/infiltrated macrophages, with the 3 microglial phenotypes activation: pro-inflammatory, immuno-regulatory and *Lgals3* and *Mrc1* anti-inflammatory markers up-regulations (Fig. 4e). Likewise, isolated GLAST-positive astrocytes develop different activation phenotypes. Both A1-specific markers (*Serping1*, *Ggta1*, *H2-D1)* and A2-specific markers (*Ptx3*, *Emp1*, *S100a10*, *Cd109*) were up-regulated (Fig. 4f). These astrocytic activation states were associated to prominent *Il6* up-regulation with a no statistically increase of *Il1b* and *Tnf* transcripts levels in DFP SE animals compared to control animals (Fig. 4f).

These results indicate important neuroinflammatory activations 24 h after DFP-induced SE. Microglial cells present pro-inflammatory, immuno-regulatory and anti-inflammatory phenotypes. At the same time point, astrocytes present 2 types of activations states: A1 and A2 activation states with joint *Il6* mRNA up-regulation.

Microglial and astrocytic activations 3 days after DFP exposure

We next studied microglial and astrocytic activations 3 days after DFP-induced SE. This time point has been widely described by others using IHC techniques and it is thought to be associated to early epileptogenesis [22]. In our model, IHC evaluation of neuroinflammation revealed marked Iba1-positive cell number increase in the 3 hippocampal regions studied (Fig. 5a and 5b). This was associated to an increase of Iba1 immunodensity in the CA3 and DG (Fig. 5a and 5c). Massive increase of GFAP immunodensity was also visible in the 3 hippocampal regions (Fig. 5a and 5d).

Quantitative RT-PCR experiments indicated marked activation of CD11B-positive isolated microglia/infiltrated macrophages. As for the 24 h time point, these cells developed 3 activation states with an increase of pro-inflammatory, immuno-regulatory and anti-inflammatory markers (Fig. 5e). Unlike the other genes, *Mrc1* was down-regulated in DFP SE animals compared to control animals (Fig. 5e). In parallel, GLAST-positive astrocytes maintained their A1 and A2-associated activation states. These 2 activations states were however not associated to an increase of *Il1b*, *Tnf* or *Il6* mRNA in DFP SE animals compared to control animals (Fig. 5f). In all, we observed that cytokines expression seemed more variable in DFP SE animals in astrocytes compared to microglia.

Taken together, these findings show frank microglial and astrocytes activation 3 days after DFP-induced SE. At this time point, the DG is particularly affected by both cell type activations. All described markers are present with an up-regulation of pro-inflammatory, immune-regulatory and anti-inflammatory markers in CD11B-positive cells and A1 and A2-associated reactive markers in GAST-positive astrocytes.

Discussion

Long lasting seizure activity and neurodegeneration induced by high doses of OPs promote neuroinflammation leading to profound pathological alterations of the brain [5, 7, 17, 20, 23]. We characterize here neuroinflammatory responses at key time points after DFP-induced SE. We confronted classical IHC analysis to RT-qPCR experiments in order to decipher microglial and astrocytic reactive markers expression and extend our understanding of SE-related neuroinflammation. Compared to RT-qPCR on cerebral tissue, RT-qPCR after cell sorting allow to identify the cellular origin of inflammatory genes up-regulation and confers increased sensibility by concentrating a specific cell type. Discussions on the existence of differential M1 and M2 phenotypes in microglial cells is still existing and M1/M2 dichotomy is certainly an oversimplification [24–27]. However diverse opposing impacts of activated microglia on neuronal damage have been demonstrated and modulation of microglial cells polarization towards a M2 phenotype have been described as beneficial [24, 25, 28–30]. Based on differential molecular markers expressions, reactive astrocytes have been also subdivided in A1 and A2 [15]. A1 astrocytes that lose most normal astrocytic functions and gain neurotoxic function are associated to multiple human and experimental models of neurological insult [31–36]. Firstly described after ischemia and postulated to be beneficial as they were associated to up-regulation of many neurotrophic factors, the impact of A2 astrocytes upon neuroinflammatory injury is mostly unclear [15, 16]. It appears that both microglia and astrocytes polarizations are greatly dependent on the type of insult and the delay after the initial insult. Our current understanding of microglia polarization after SE is limited and astrocyte polarization has yet not been studied. Our study reveals sequential activations of microglial and astrocytic phenotypes.

As soon as 1 h post DFP injection, corresponding to 40 min of SE [17], we observe an early pro-inflammatory phenotype in microglia. Previous studies demonstrated that 30–40 min of SE was associated to benzodiazepine-refractoriness in different SE models [9, 19–21, 37–39]. It has been shown that the pro-inflammatory cytokine IL1β could play an important role in benzodiazepine response in SE

induced by intrahippocampal injection of KA as IL-1β icv injection prolonged diazepam latency to terminate SE [9]. Furthermore, in this project, SE was responsive to diazepam at 40 min in *Il1r1* knock-out mice compared to WT mice [9]. Our results show that, at this very early stage, *Il1b* mRNA increase is associated to microglia. At the same stage, neurotoxic A1 astrocytic activation is still absent, in accordance with the idea that pro-inflammatory microglia activation precedes pro-inflammatory astrocyte activation [40]. However, at this early time point, we observed an A2-associated reactive phenotype with the up-regulation of *Ptgs2*, coding for Cox2 protein, and *Ptx3* mRNA. Our results further show that this up-regulation of A2-associated markers is concomitant to an *Il6* increase. Expression of Il6 protein has been described in astrocytes 12 and 24 h after soman-induced SE in rats, but Il6 presence has not been studied at earlier stages [41]. IL6 is a pleiotropic cytokine, modulating the inflammatory response by exerting both protective and detrimental activities in neuronal tissue. Il6 icv injection has been shown to induce epileptogenesis with the occurrence of cortical seizures detected 3 days after the injection in a dose-dependent manner in C57Bl6 mice [42]. Although A2 astrocytes are thought to be beneficial, A2 astrocytes expressing Cox2 have been proposed as deleterious on oligodendrocyte progenitor cells maturation in a mouse model of neonatal white matter injury [43]. Overall, we described for the first time the early A2 activation phenotype of astrocytes after SE, and its implication in SE maintenance and neuronal degeneration has to be further assessed.

Using the same techniques, while 4 h after DFP injection no modifications were still noticeable by IHC, we observed an up-regulation of pro-inflammatory and immuno-regulatory markers in microglial cells. Interestingly, this time point is associated to a significant increase of *Il1rn* mRNA, which will persist up to 3 days post-injection, with a \tilde 270 fold increase at 24 h (Table 1). IL1RA protein, encoded by *IL1RN*, binds the receptor IL1R1 and blocks IL1α and IL1β signaling. IL1β-IL1R1 signaling has been widely implicated in seizures occurrence and epileptogenesis (for review, [8, 44, 45]) and IL1β-IL1R1 signaling blockade has been shown to reduce seizure number, neurodegeneration and epileptogenesis [46–50]. In this regard, soman-induced SE was accompanied with a mild increase of neurodegeneration in *Il1r1* and *Il1rn* knock-out mice but SE duration and severity have not been studied with EEG [51]. We did not observe *Il1b* mRNA up-regulation in isolated astrocytes at any time points. This is in accordance with the exclusive expression of Il1β at a protein level in activated microglia 24 h after soman-induced SE [41]. Astrocytic expression of Il1β is observed later in time from 4 days [52] in pilocarpine SE model, but discrepancies exist as Il1β has been observed in astrocytes earlier in the pilocarpine model by others [53] or other types of seizures [54–56].

At 24 h after DFP-induced SE, in accordance with the massive neurodegeneration observed in our model [17], both microglial and astrocytic activations were visualized by IHC analysis. In CD11B-positive isolated cells, while pro-inflammatory and immuno-regulatory markers were maintained, anti-inflammatory markers appeared up-regulated. This time point was associated to a \tilde 72 fold increase of the *Lgals3* mRNA, this increase persisting at 3 days post-SE (Table 1). Galectin-3 protein, encoded by *Lgals3*, released by microglia, plays a pivotal role in phagocytosis by binding targeted cells or bacteria [57]. Galectin-3-positive microglia were observed to engulf degenerative neurons in a model of ischemia

by middle cerebral artery occlusion [55]. Furthermore, in this model *Lgals3* knock-out mice presented increased cell death, suggesting a protective role of Galectin-3 after ischemia [58]. Although, *Lgals3* mRNA is strongly up-regulated in microglia after pilocarpine-induced SE, *Lgals3* knock-out mice presented a small reduction of cell death in the cortex and no difference in the hippocampus 3 days after pilocarpine injection compared to WT mice, suggesting that, after SE, Galectin-3 protective role is more marginal [59]. Meanwhile, in GLAST-positive isolated cells, while A2-specific markers were maintained, A1-specific markers appeared up-regulated for the first time after DFP exposure. The role of neurotoxic astrogliosis in neurodegeneration has been demonstrated and different mechanisms have been identified, such as, reduced glutamate clearance, adenosine cycle modifications, increased Ca^{2+} signaling and BBB dysfunction [60].

Finally, 3 days after DFP injection, corresponding to early epileptogenesis, previous works have observed strong neuroinflammation in different models of SE [21, 36, 61–63]. In our model, we observed a significant increase in Iba1-positive cell number in all hippocampal regions. This increase was already noticeable at 24 h but increased with time (Table 1). In a SE model induced by icv infusion of KA, Feng and colleagues have observed microglial proliferation and macrophages infiltration at both 24 h and 3 days SE [65]. As the Iba1 marker do not permit to differentiate microglial and infiltrated macrophages, we cannot state if the increases of Iba1-positive cells observed at 24 h and 3 days are due to microglia migration, proliferation or macrophages infiltration. Further work is needed to address this issue in our model. At this time point, in pilocarpine SE model, pro-inflammatory (M1-like) and anti-inflammatory microglial phenotypes (M2a-like) have been observed in the forebrain [64]. However, in SE model induced by intrahippocampal KA, the anti-inflammatory phenotype was not observed at the same time point, showing that models specificities exist [64].

Conclusions

Our work identified sequential microglial and astrocytic phenotypes activations. Given the very early neuroinflammatory modifications observed, targeting these modifications could be a beneficial strategy for the treatment of refractory SE and its cerebral consequences. This type of intervention should probably be provided very early in the course of the SE. Further comprehensive study of A2 reactive astrocytes role in SE is nevertheless needed. An adapted treatment paradigm in order to address specific phases of neuroinflammation could increase therapeutic impact.

Abbreviations

AChE
acetylcholinesterase
AS
atropine sulfate
CA1
cornu ammonis 1

CA3
cornu ammonis 3
ChEs
cholinesterases
DFP
Diisopropylfluorophosphate
DG
dentate gyrus
HI-6
asoxime
icv
intracerebroventricular
IHC
immunohistochemistry
ip
intraperitoneal
KA
kainate
OPs
organophosphate compounds
sc
subcutaneous
SE
status epilepticus
SRBD
seizure-related brain damage
WT
wild type

Declarations

Ethics approval and consent to participate

A statement on ethics for the experiments involving animals is included in the manuscript.

Consent for publication

Not applicable

Availability of data and materials

The datasets used and/or analyzed during the current study are available from the corresponding author on reasonable request.

Competing interests

The authors declare that they have no competing interests.

Funding

This work was supported by the French Ministry of Armed Forces: Direction Générale de l'Armement (DGA) and Service de Santé des Armées (SSA). Funding sources had no involvement in study design, collection, analysis or interpretation of data, or decision to publish.

Authors' contributions

C.M, J.E, N.D performed the experiments, the analysis and designed the figures. R.H.A and A.I. helped carry out the experiments. N.D. developed the study design, supervised the project and wrote the manuscript. S.A., N.S.Y, X.B, F.N, G.D contributed to the final manuscript.

Acknowledgments

This work used the imagery platform of IRBA supported by the Service de Santé des Armées. We particularly thank Mr. X. Butigieg for technical support.

Authors' information

Not applicable

References

1. Auvin S, Dupuis N. Outcome of status epilepticus. What do we learn from animal data? Epileptic Disord. 2014;16(Spec No 1):37–43.
2. Hamilton SE, Loose MD, Qi M, Levey AI, Hille B, McKnight GS, et al. Disruption of the m1 receptor gene ablates muscarinic receptor-dependent M current regulation and seizure activity in mice. Proc Natl Acad Sci USA. 1997;94:13311–6.
3. Chen JWY, Wasterlain CG. Status epilepticus: pathophysiology and management in adults. Lancet Neurol. 2006;5:246–56.
4. Baille V, Clarke PGH, Brochier G, Dorandeu F, Verna J-M, Four E, et al. Soman-induced convulsions: the neuropathology revisited. Toxicology. 2005;215:1–24.
5. Deshpande LS, Blair RE, Huang BA, Phillips KF, DeLorenzo RJ. Pharmacological blockade of the calcium plateau provides neuroprotection following organophosphate paraoxon induced status epilepticus in rats. Neurotoxicol Teratol. 2016;56:81–6.

6. Li Y, Lein PJ, Liu C, Bruun DA, Tewolde T, Ford G, et al. Spatiotemporal pattern of neuronal injury induced by DFP in rats: a model for delayed neuronal cell death following acute OP intoxication. Toxicol Appl Pharmacol. 2011;253:261–9.
7. McDonough JH, Shih TM. Neuropharmacological mechanisms of nerve agent-induced seizure and neuropathology. Neurosci Biobehav Rev. 1997;21:559–79.
8. Vezzani A, Balosso S, Ravizza T. Neuroinflammatory pathways as treatment targets and biomarkers in epilepsy. Nat Rev Neurol. 2019;15:459–72.
9. Xu Z-H, Wang Y, Tao A-F, Yu J, Wang X-Y, Zu Y-Y, et al. Interleukin-1 receptor is a target for adjunctive control of diazepam-refractory status epilepticus in mice. Neuroscience. 2016;328:22–9.
10. Sankar R, Auvin S, Mazarati A, Shin D. Inflammation contributes to seizure-induced hippocampal injury in the neonatal rat brain. Acta Neurol Scand. 2007;115:16–20.
11. Auvin S, Shin D, Mazarati A, Sankar R. Inflammation induced by LPS enhances epileptogenesis in immature rat and may be partially reversed by IL1RA. Epilepsia. 2010;51(Suppl 3):34–8.
12. Chhor V, Le Charpentier T, Lebon S, Oré M-V, Celador IL, Josserand J, et al. Characterization of phenotype markers and neuronotoxic potential of polarised primary microglia in vitro. Brain Behav Immun. 2013;32:70–85.
13. Colton CA. Heterogeneity of microglial activation in the innate immune response in the brain. J Neuroimmune Pharmacol. 2009;4:399–418.
14. Prinz M, Priller J, Sisodia SS, Ransohoff RM. Heterogeneity of CNS myeloid cells and their roles in neurodegeneration. Nat Neurosci. 2011;14:1227–35.
15. Liddelow SA, Guttenplan KA, Clarke LE, Bennett FC, Bohlen CJ, Schirmer L, et al. Neurotoxic reactive astrocytes are induced by activated microglia. Nature. 2017;541:481–7.
16. Zamanian JL, Xu L, Foo LC, Nouri N, Zhou L, Giffard RG, et al. Genomic analysis of reactive astrogliosis. J Neurosci. 2012;32:6391–410.
17. Enderlin J, Igert A, Auvin S, Nachon F, Dal Bo G, Dupuis N. Characterization of organophosphate-induced brain injuries in a convulsive mouse model of diisopropylfluorophosphate exposure. Epilepsia. 2020;61:e54–9.
18. Rideau Batista Novais A, Pham H, Van de Looij Y, Bernal M, Mairesse J, Zana-Taieb E, et al. Transcriptomic regulations in oligodendroglial and microglial cells related to brain damage following fetal growth restriction. Glia. 2016;64:2306–20.
19. Mazarati AM, Baldwin RA, Sankar R, Wasterlain CG. Time-dependent decrease in the effectiveness of antiepileptic drugs during the course of self-sustaining status epilepticus. Brain Res. 1998;814:179–85.
20. Todorovic MS, Cowan ML, Balint CA, Sun C, Kapur J. Characterization of status epilepticus induced by two organophosphates in rats. Epilepsy Res. 2012;101:268–76.
21. Wu X, Kuruba R, Reddy DS. Midazolam-Resistant Seizures and Brain Injury after Acute Intoxication of Diisopropylfluorophosphate, an Organophosphate Pesticide and Surrogate for Nerve Agents. J

Pharmacol Exp Ther. 2018;367:302–21.

22. Vezzani A, Lang B, Aronica E. Immunity and Inflammation in Epilepsy. Cold Spring Harb Perspect Med. 2015;6:a022699.
23. de Araujo Furtado M, Rossetti F, Chanda S, Yourick D. Exposure to nerve agents: from status epilepticus to neuroinflammation, brain damage, neurogenesis and epilepsy. Neurotoxicology. 2012;33:1476–90.
24. Chu X, Cao L, Yu Z, Xin D, Li T, Ma W, et al. Hydrogen-rich saline promotes microglia M2 polarization and complement-mediated synapse loss to restore behavioral deficits following hypoxia-ischemic in neonatal mice via AMPK activation. J Neuroinflammation. 2019;16:104.
25. Liu J-T, Wu S-X, Zhang H, Kuang F. Inhibition of MyD88 Signaling Skews Microglia/Macrophage Polarization and Attenuates Neuronal Apoptosis in the Hippocampus After Status Epilepticus in Mice. Neurotherapeutics. 2018;15:1093–111.
26. Yuan Y, Wu C, Ling E-A. Heterogeneity of Microglia Phenotypes: Developmental, Functional and Some Therapeutic Considerations. Curr Pharm Des. 2019;25:2375–93.
27. Ransohoff RM. A polarizing question: do M1 and M2 microglia exist? Nat Neurosci. 2016;19:987–91.
28. Xu X, Gao W, Cheng S, Yin D, Li F, Wu Y, et al. Anti-inflammatory and immunomodulatory mechanisms of atorvastatin in a murine model of traumatic brain injury. J Neuroinflammation. 2017;14:167.
29. Kong W, Hooper KM, Ganea D. The natural dual cyclooxygenase and 5-lipoxygenase inhibitor flavocoxid is protective in EAE through effects on Th1/Th17 differentiation and macrophage/microglia activation. Brain Behav Immun. 2016;53:59–71.
30. Li T, Zhai X, Jiang J, Song X, Han W, Ma J, et al. Intraperitoneal injection of IL-4/IFN-γ modulates the proportions of microglial phenotypes and improves epilepsy outcomes in a pilocarpine model of acquired epilepsy. Brain Res. 2017;1657:120–9.
31. Aronica E, Ravizza T, Zurolo E, Vezzani A. Astrocyte immune responses in epilepsy. Glia. 2012;60:1258–68.
32. Aronica E, Crino PB. Inflammation in epilepsy: clinical observations. Epilepsia. 2011;52(Suppl 3):26–32.
33. Steinhäuser C, Seifert G. Astrocyte dysfunction in epilepsy. In: Noebels JL, Avoli M, Rogawski MA, Olsen RW, Delgado-Escueta AV, editors. Jasper's Basic Mechanisms of the Epilepsies [Internet]. 4th ed. Bethesda (MD): National Center for Biotechnology Information (US); 2012 [cited 2020 Jul 30]. Available from: http://www.ncbi.nlm.nih.gov/books/NBK98180/.
34. Vezzani A, Ravizza T, Balosso S, Aronica E. Glia as a source of cytokines: implications for neuronal excitability and survival. Epilepsia. 2008;49(Suppl 2):24–32.
35. Sofroniew MV, Vinters HV. Astrocytes: biology and pathology. Acta Neuropathol. 2010;119:7–35.
36. Liu C, Li Y, Lein PJ, Ford BD. Spatiotemporal patterns of GFAP upregulation in rat brain following acute intoxication with diisopropylfluorophosphate (DFP). Curr Neurobiol. 2012;3:90–7.

37. Wasterlain CG, Liu H, Naylor DE, Thompson KW, Suchomelova L, Niquet J, et al. Molecular basis of self-sustaining seizures and pharmacoresistance during status epilepticus: The receptor trafficking hypothesis revisited. Epilepsia. 2009;50(Suppl 12):16–8.
38. Kapur J, Macdonald RL. Rapid seizure-induced reduction of benzodiazepine and Zn2 + sensitivity of hippocampal dentate granule cell GABAA receptors. J Neurosci. 1997;17:7532–40.
39. Kuruba R, Wu X, Reddy DS. Benzodiazepine-refractory status epilepticus, neuroinflammation, and interneuron neurodegeneration after acute organophosphate intoxication. Biochim Biophys Acta Mol Basis Dis. 2018;1864:2845–58.
40. Liddelow SA, Guttenplan KA, Clarke LE, Bennett FC, Bohlen CJ, Schirmer L, et al. Neurotoxic reactive astrocytes are induced by activated microglia. Nature. 2017;541:481–7.
41. Johnson EA, Kan RK. The acute phase response and soman-induced status epilepticus: temporal, regional and cellular changes in rat brain cytokine concentrations. J Neuroinflammation. 2010;7:40.
42. Levy N, Milikovsky DZ, Baranauskas G, Vinogradov E, David Y, Ketzef M, et al. Differential TGF-β Signaling in Glial Subsets Underlies IL-6-Mediated Epileptogenesis in Mice. J Immunol. 2015;195:1713–22.
43. Shiow LR, Favrais G, Schirmer L, Schang A-L, Cipriani S, Andres C, et al. Reactive astrocyte COX2-PGE2 production inhibits oligodendrocyte maturation in neonatal white matter injury. Glia. 2017;65:2024–37.
44. Vezzani A, Maroso M, Balosso S, Sanchez M-A, Bartfai T. IL-1 receptor/Toll-like receptor signaling in infection, inflammation, stress and neurodegeneration couples hyperexcitability and seizures. Brain Behav Immun. 2011;25:1281–9.
45. van Vliet EA, Aronica E, Vezzani A, Ravizza T. Review. Neuroinflammatory pathways as treatment targets and biomarker candidates in epilepsy: emerging evidence from preclinical and clinical studies. Neuropathol Appl Neurobiol. 2018;44:91–111.
46. Vezzani A, Balosso S, Maroso M, Zardoni D, Noé F, Ravizza T. ICE/caspase 1 inhibitors and IL-1beta receptor antagonists as potential therapeutics in epilepsy. Curr Opin Investig Drugs. 2010;11:43–50.
47. Maroso M, Balosso S, Ravizza T, Liu J, Aronica E, Iyer AM, et al. Toll-like receptor 4 and high-mobility group box-1 are involved in ictogenesis and can be targeted to reduce seizures. Nat Med. 2010;16:413–9.
48. Iori V, Iyer AM, Ravizza T, Beltrame L, Paracchini L, Marchini S, et al. Blockade of the IL-1R1/TLR4 pathway mediates disease-modification therapeutic effects in a model of acquired epilepsy. Neurobiol Dis. 2017;99:12–23.
49. Noe FM, Polascheck N, Frigerio F, Bankstahl M, Ravizza T, Marchini S, et al. Pharmacological blockade of IL-1β/IL-1 receptor type 1 axis during epileptogenesis provides neuroprotection in two rat models of temporal lobe epilepsy. Neurobiol Dis. 2013;59:183–93.
50. Vezzani A, Moneta D, Conti M, Richichi C, Ravizza T, De Luigi A, et al. Powerful anticonvulsant action of IL-1 receptor antagonist on intracerebral injection and astrocytic overexpression in mice. Proc Natl Acad Sci USA. 2000;97:11534–9.

51. Ferrara-Bowens TM, Chandler JK, Guignet MA, Irwin JF, Laitipaya K, Palmer DD, et al. Neuropathological and behavioral sequelae in IL-1R1 and IL-1Ra gene knockout mice after soman (GD) exposure. Neurotoxicology. 2017;63:43–56.
52. Vinet J, Vainchtein ID, Spano C, Giordano C, Bordini D, Curia G, et al. Microglia are less pro-inflammatory than myeloid infiltrates in the hippocampus of mice exposed to status epilepticus. Glia. 2016;64:1350–62.
53. Ravizza T, Gagliardi B, Noé F, Boer K, Aronica E, Vezzani A. Innate and adaptive immunity during epileptogenesis and spontaneous seizures: evidence from experimental models and human temporal lobe epilepsy. Neurobiol Dis. 2008;29:142–60.
54. Balosso S, Maroso M, Sanchez-Alavez M, Ravizza T, Frasca A, Bartfai T, et al. A novel non-transcriptional pathway mediates the proconvulsive effects of interleukin-1beta. Brain. 2008;131:3256–65.
55. Akin D, Ravizza T, Maroso M, Carcak N, Eryigit T, Vanzulli I, et al. IL-1β is induced in reactive astrocytes in the somatosensory cortex of rats with genetic absence epilepsy at the onset of spike-and-wave discharges, and contributes to their occurrence. Neurobiol Dis. 2011;44:259–69.
56. Ravizza T, Noé F, Zardoni D, Vaghi V, Sifringer M, Vezzani A. Interleukin Converting Enzyme inhibition impairs kindling epileptogenesis in rats by blocking astrocytic IL-1beta production. Neurobiol Dis. 2008;31:327–33.
57. Cockram TOJ, Puigdellívol M, Brown GC. Calreticulin and Galectin-3 Opsonise Bacteria for Phagocytosis by Microglia. Front Immunol. 2019;10:2647.
58. Lalancette-Hébert M, Swarup V, Beaulieu JM, Bohacek I, Abdelhamid E, Weng YC, et al. Galectin-3 is required for resident microglia activation and proliferation in response to ischemic injury. J Neurosci. 2012;32:10383–95.
59. Bischoff V, Deogracias R, Poirier F, Barde Y-A. Seizure-induced neuronal death is suppressed in the absence of the endogenous lectin Galectin-1. J Neurosci. 2012;32:15590–600.
60. Noebels JL, Avoli M, Rogawski MA, Olsen RW, Delgado-Escueta AV, editors. Jasper's Basic Mechanisms of the Epilepsies [Internet]. 4th ed. Bethesda (MD): National Center for Biotechnology Information (US); 2012 [cited 2020 Jul 27]. Available from: http://www.ncbi.nlm.nih.gov/books/NBK50785/.
61. Dhote F, Peinnequin A, Carpentier P, Baille V, Delacour C, Foquin A, et al. Prolonged inflammatory gene response following soman-induced seizures in mice. Toxicology. 2007;238:166–76.
62. Collombet J-M, Four E, Bernabé D, Masqueliez C, Burckhart M-F, Baille V, et al. Soman poisoning increases neural progenitor proliferation and induces long-term glial activation in mouse brain. Toxicology. 2005;208:319–34.
63. Schartz ND, Herr SA, Madsen L, Butts SJ, Torres C, Mendez LB, et al. Spatiotemporal profile of Map2 and microglial changes in the hippocampal CA1 region following pilocarpine-induced status epilepticus. Sci Rep. 2016;6:24988.

64. Benson MJ, Manzanero S, Borges K. Complex alterations in microglial M1/M2 markers during the development of epilepsy in two mouse models. Epilepsia. 2015;56:895–905.
65. Feng L, Murugan M, Bosco DB, Liu Y, Peng J, Worrell GA, et al. Microglial proliferation and monocyte infiltration contribute to microgliosis following status epilepticus. Glia. 2019;67:1434–48.

Tables

Due to technical limitations, table 1 is only available as a download in the Supplemental Files section.

Figures

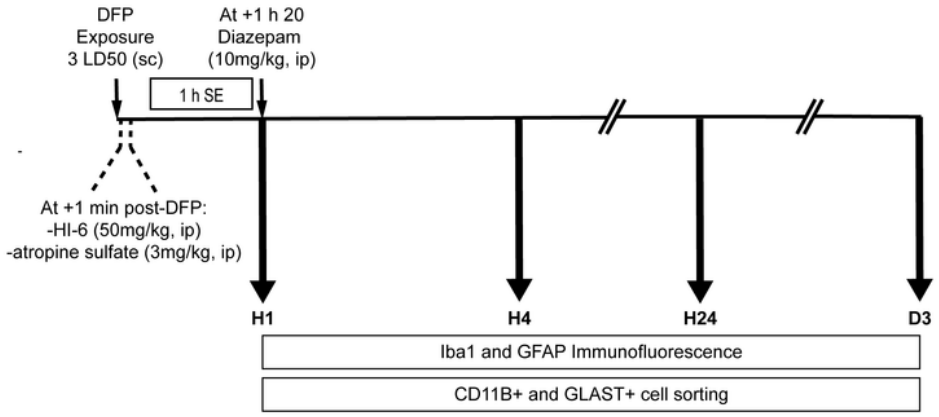

Figure 1

DFP exposure protocol. Mice received an injection of DFP (3 LD50 = 9.93mg/kg, LD50 calculated without HI-6 and AS post-treatment, 10ml/kg, s.c.) followed by combined i.p. injection of HI-6 (50mg/kg) and atropine sulfate (3mg/kg) at +1 min of DFP injection. HI-6 and AS post-treatment is used to reduce respiratory distress and mortality. Except for the 1 h experimental group, all animals received Diazepam (10mg/kg, i.p.), eighty minutes after DFP injection, corresponding to 1 h long SE. Control animals received

all treatments after vehicle injection without DFP. Iba1 and GFAP immunofluorescences, as CD11B+ and GLAST+ cell sortings were conducted 1 h, 4 h, 24 h and 3 d post-DFP injection. ip, intraperitoneal; sc, subcutaneous.

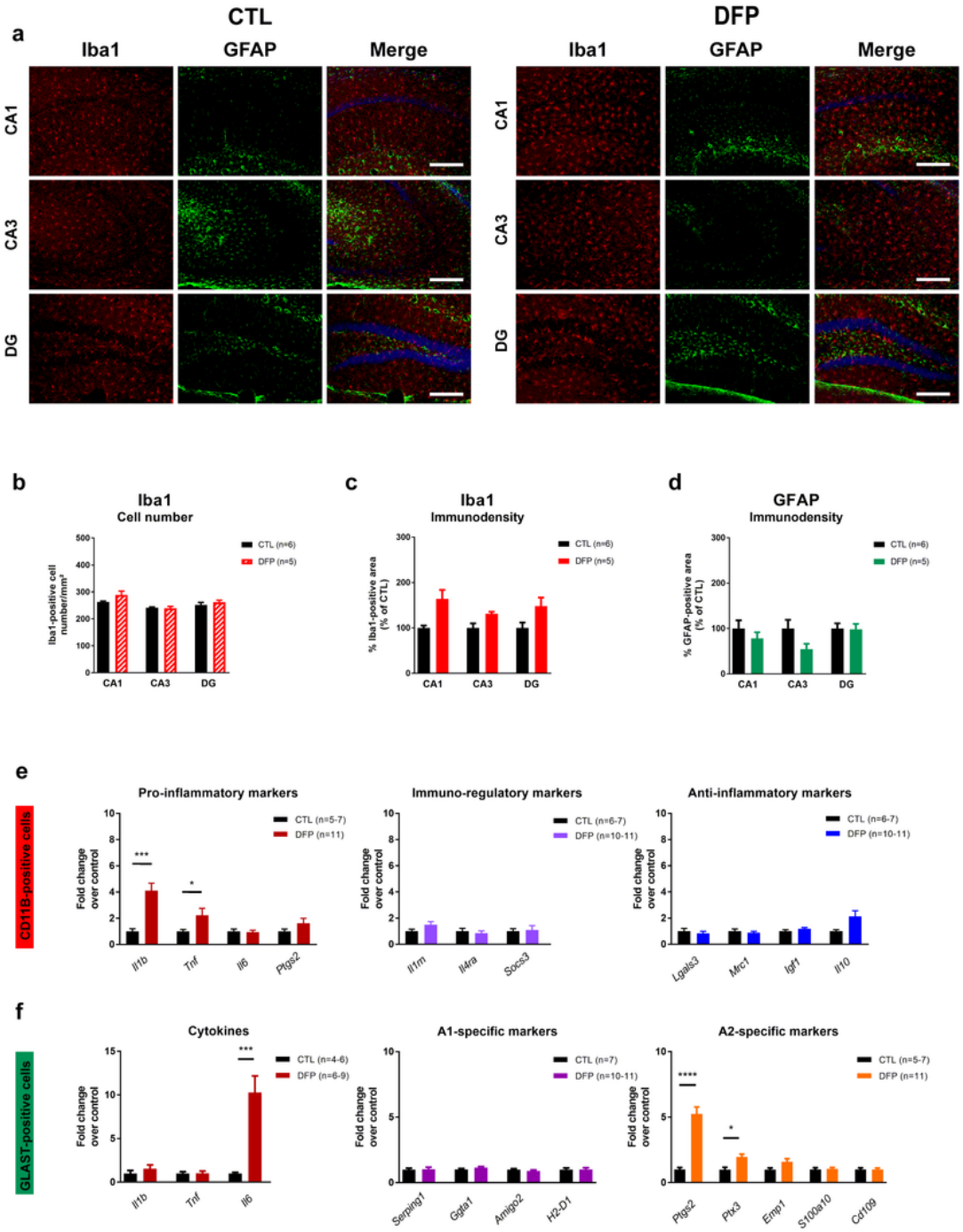

Figure 2

Neuroinflammatory response 1 hour after DFP exposure. a Immunohistochemical detection of the microglial/macrophage marker Iba1 (red) and the astrocytic marker GFAP (green) in CA1, CA3 and DG

hippocampal regions of control (CTL) and DFP SE mice. b Iba1-positive cell number, c Iba1-postitive immunodensity and d GFAP immunodensity in in CA1, CA3 and DG hippocampal regions of control (CTL) and DFP SE mice. e Quantitative RT-PCR analysis of pro-inflammatory (Il1b, Tnf, Il6, Ptgs2), immuno-regulatory (Il1rn, Il4ra, Socs3) and anti-inflammatory (Lgals3, Mrc1, Igf1, Il10) markers in isolated CD11B-positive cells of control (CTL) and DFP SE brains. Quantitative RT-PCR analysis of cytokines (Il1b, Tnf, Il6), A1-associated reactive (Serping1, Ggta1, Amigo2, H2-D1) and A2-associated reactive (Ptgs2, Ptx3, Emp1, S100a10, Cd109) markers in isolated GLAST-positive cells of control (CTL) and DFP SE brains. *p < 0.05, **p <0.01, ***p < 0.001, ****p < 0.0001 vs CTL (Mann-Whitney test). Data are presented as mean ± SEM. Scale bar = 200μm.

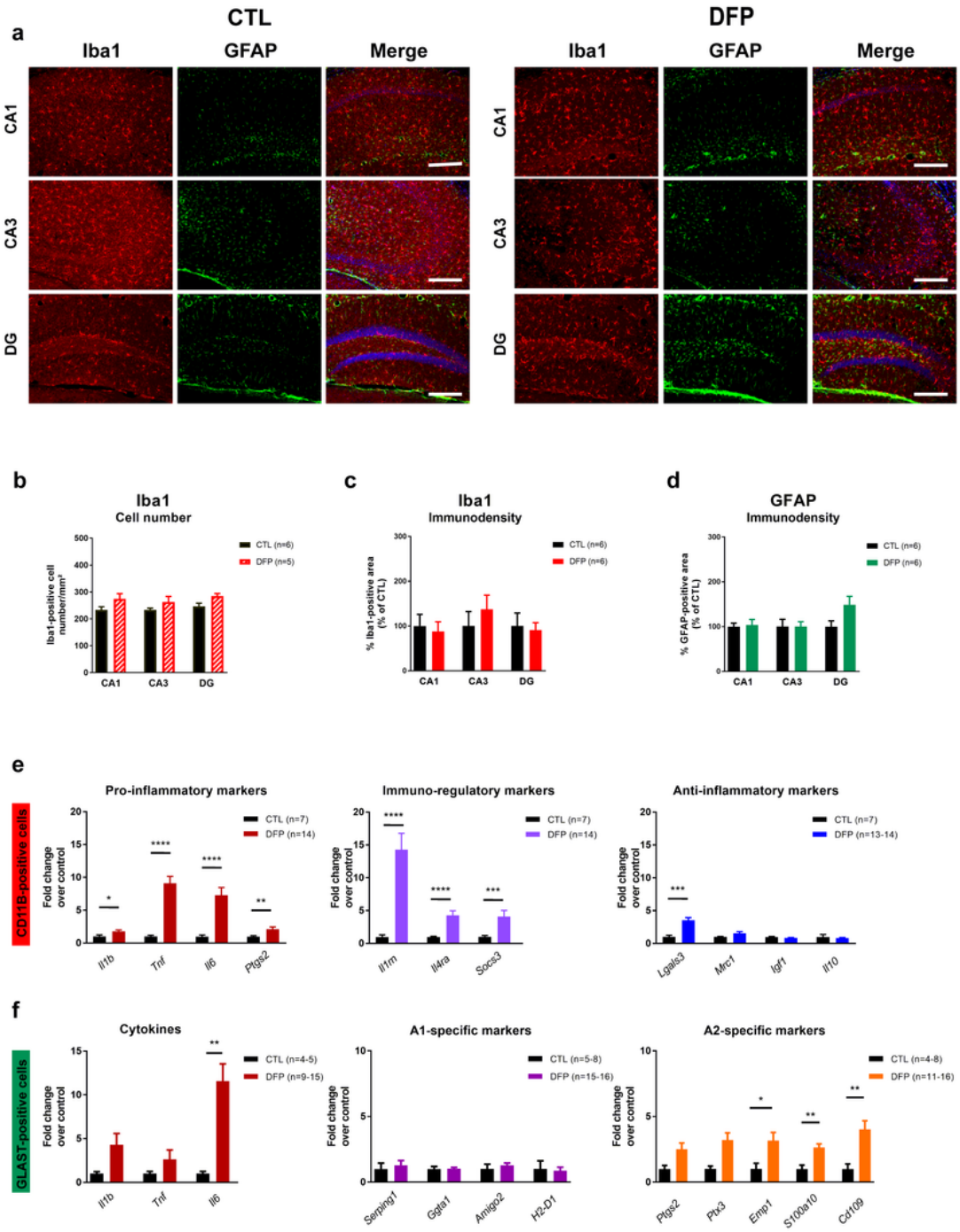

Figure 3

Neuroinflammatory response 4 hours after DFP exposure. a Immunohistochemical detection of the microglial/macrophage marker Iba1 (red) and the astrocytic marker GFAP (green) in CA1, CA3 and DG hippocampal regions of control (CTL) and DFP SE mice. b Iba1-positive cell number, c Iba1-postitive immunodensity and d GFAP immunodensity in in CA1, CA3 and DG hippocampal regions of control (CTL) and DFP SE mice. e Quantitative RT-PCR analysis of pro-inflammatory (Il1b, Tnf, Il6, Ptgs2), immuno-

regulatory (Il1rn, Il4ra, Socs3) and anti-inflammatory (Lgals3, Mrc1, Igf1, Il10) markers in isolated CD11B-positive cells of control (CTL) and DFP SE brains. Quantitative RT-PCR analysis of cytokines (Il1b, Tnf, Il6), A1-associated reactive (Serping1, Ggta1, Amigo2, H2-D1) and A2-associated reactive (Ptgs2, Ptx3, Emp1, S100a10, Cd109) markers in isolated GLAST-positive cells of control (CTL) and DFP SE brains. *p < 0.05, **p <0.01, ***p < 0.001, ****p < 0.0001 vs CTL (Mann-Whitney test). Data are presented as mean ± SEM. Scale bar = 200µm.

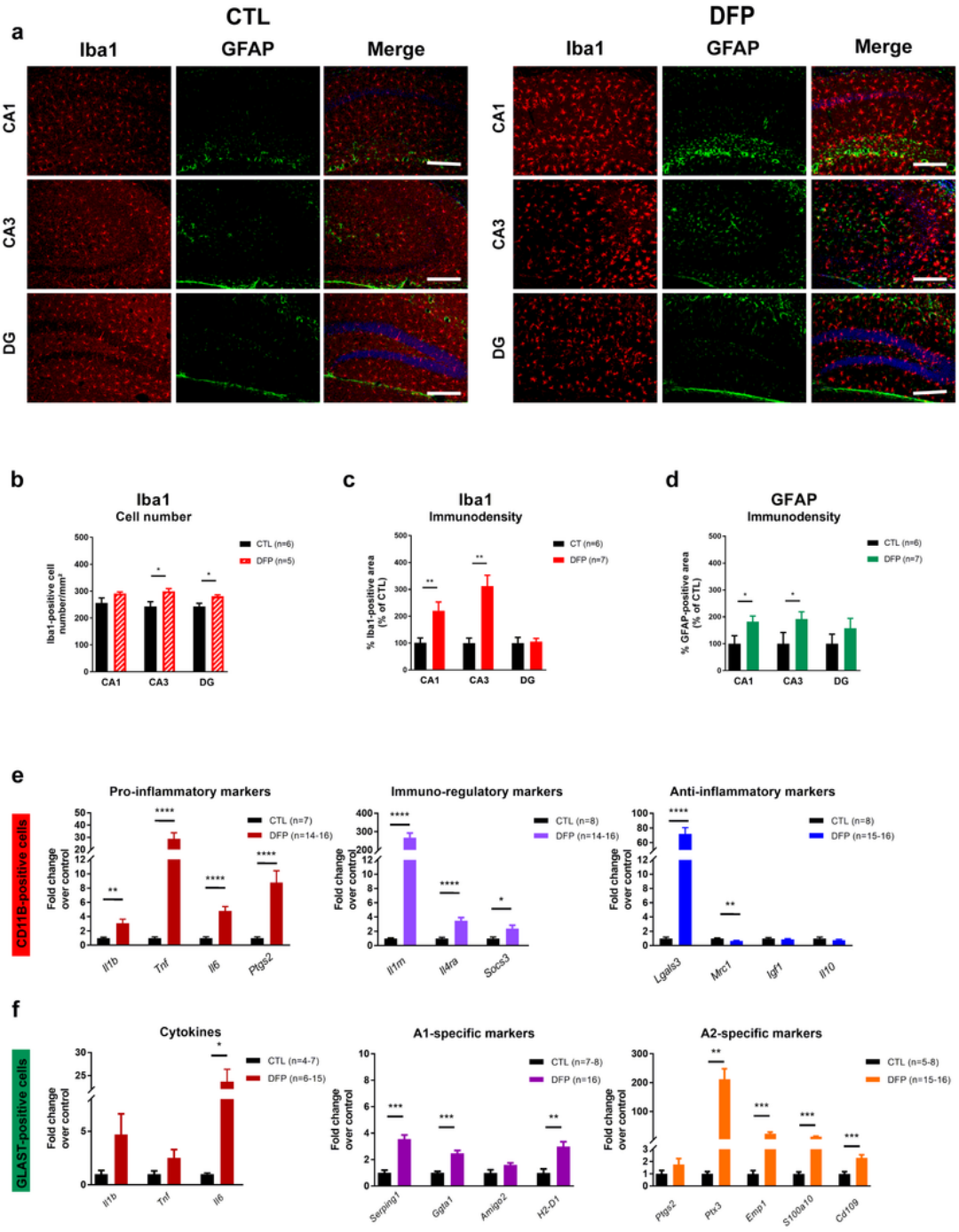

Figure 4

Neuroinflammatory response 24 hours after DFP exposure. a Immunohistochemical detection of the microglial/macrophage marker Iba1 (red) and the astrocytic marker GFAP (green) in CA1, CA3 and DG hippocampal regions of control (CTL) and DFP SE mice. b Iba1-positive cell number, c Iba1-postitive immunodensity and d GFAP immunodensity in in CA1, CA3 and DG hippocampal regions of control (CTL) and DFP SE mice. e Quantitative RT-PCR analysis of pro-inflammatory (Il1b, Tnf, Il6, Ptgs2), immuno-regulatory (Il1rn, Il4ra, Socs3) and anti-inflammatory (Lgals3, Mrc1, Igf1, Il10) markers in isolated CD11B-positive cells of control (CTL) and DFP SE brains. Quantitative RT-PCR analysis of cytokines (Il1b, Tnf, Il6), A1-associated reactive (Serping1, Ggta1, Amigo2, H2-D1) and A2-associated reactive (Ptgs2, Ptx3, Emp1, S100a10, Cd109) markers in isolated GLAST-positive cells of control (CTL) and DFP SE brains. *p < 0.05, **p <0.01, ***p < 0.001, ****p < 0.0001 vs CTL (Mann-Whitney test). Data are presented as mean ± SEM. Scale bar = 200µm.

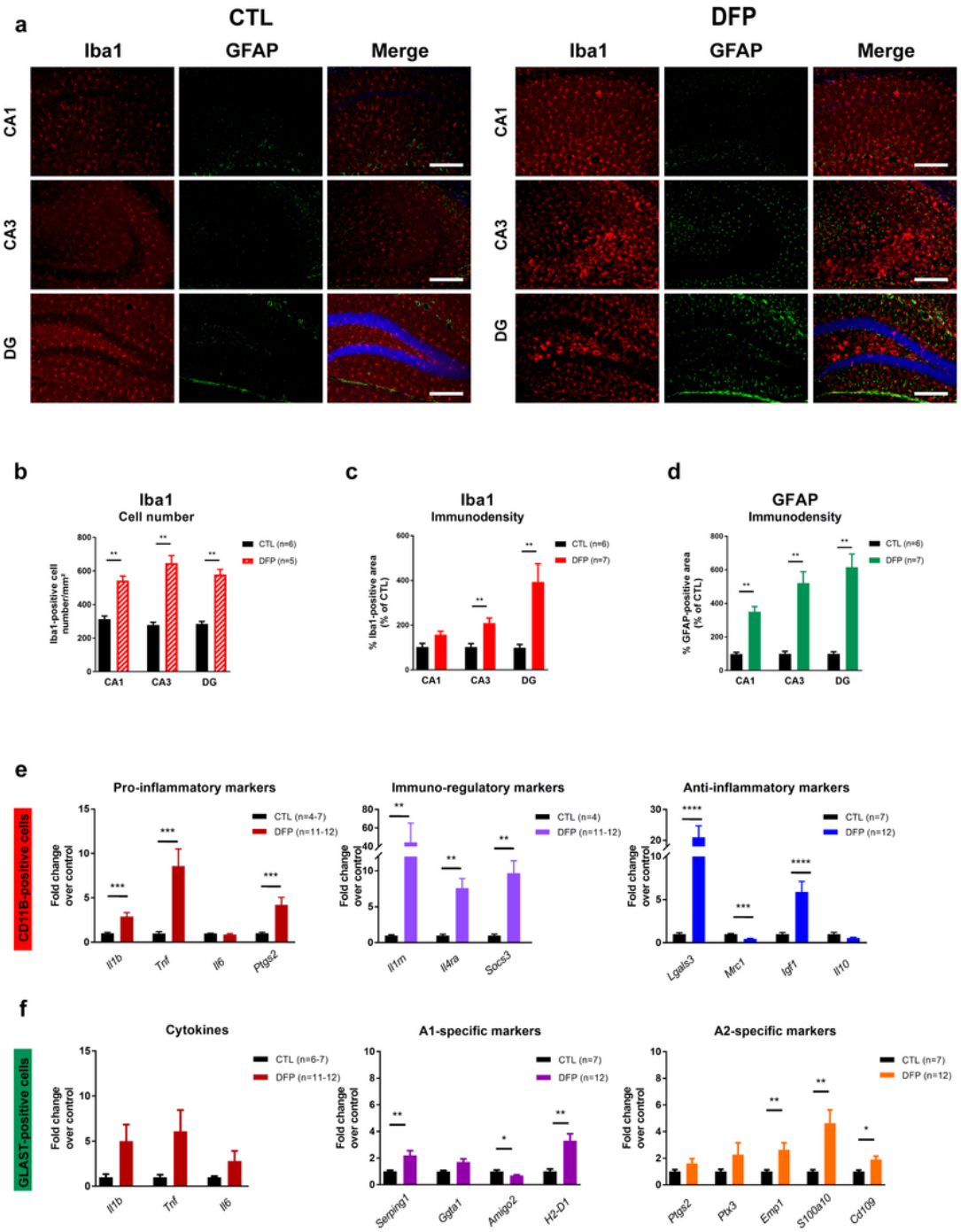

Figure 5

Neuroinflammatory response 3 days after DFP exposure. a Immunohistochemical detection of the microglial/macrophage marker Iba1 (red) and the astrocytic marker GFAP (green) in CA1, CA3 and DG hippocampal regions of control (CTL) and DFP SE mice. b Iba1-positive cell number, c Iba1-postitive immunodensity and d GFAP immunodensity in in CA1, CA3 and DG hippocampal regions of control (CTL) and DFP SE mice. e Quantitative RT-PCR analysis of pro-inflammatory (Il1b, Tnf, Il6, Ptgs2), immuno-

regulatory (Il1rn, Il4ra, Socs3) and anti-inflammatory (Lgals3, Mrc1, Igf1, Il10) markers in isolated CD11B-positive cells of control (CTL) and DFP SE brains. Quantitative RT-PCR analysis of cytokines (Il1b, Tnf, Il6), A1-associated reactive (Serping1, Ggta1, Amigo2, H2-D1) and A2-associated reactive (Ptgs2, Ptx3, Emp1, S100a10, Cd109) markers in isolated GLAST-positive cells of control (CTL) and DFP SE brains. *p < 0.05, **p <0.01, ***p < 0.001, ****p < 0.0001 vs CTL (Mann-Whitney test). Data are presented as mean ± SEM. Scale bar = 200µm.

Supplementary Files

This is a list of supplementary files associated with this preprint. Click to download.

- Table1Maupuetal.tif
- Table1Maupuetal.tif
- SupplementaryInformationMaupuetal.docx
- SupplementaryInformationMaupuetal.docx
- ManuscriptMaupuetal.pdf
- ManuscriptMaupuetal.pdf